

# Doubly-Fed Generator Control using two Different Types of Controllers

Rayane LEULMI<sup>1</sup>, Salima LEKHCHINE<sup>2</sup>, Ammar MEDOUE<sup>1</sup>

<sup>1</sup> Department of Electrical Engineering, LES Laboratory,  
University of 20 August 1955-Skikda, Algeria.

<sup>2</sup> Department of Electrical Engineering, LGMM Laboratory,  
University of 20 August 1955-Skikda, Algeria.

E-mail : [rayane.leulmi@univ-skikda.dz](mailto:rayane.leulmi@univ-skikda.dz), [slekhchine@yahoo.fr](mailto:slekhchine@yahoo.fr), [amedoud75@yahoo.fr](mailto:amedoud75@yahoo.fr)

**Abstract** — In our daily lives, the world's economy is based on two different forms of energy: non-renewable energy such as oil and nuclear power, and renewable energy such as photovoltaic and wind power. Non-renewable energy has many negative impacts on mankind and the environment, which is why researchers have found another energy source for the world's economy. However, renewable energies offer many advantages for mankind. One of the best-known sources is wind power. Wind energy transforms wind energy into mechanical or electrical energy. This work presents the description and modeling of wind energy production systems based on a doubly-fed generator. The work highlights a maximum power point tracking technique with speed control to achieve the objective of optimal operation and better utilization of the wind turbine. Two different speed control methods are presented: a classical proportional-integral controller and an advanced backstepping controller. At the end of the modeling and simulation of the system in the MATLAB/Simulink environment, the analysis of the results shows good performance.

**Keywords** — Wind energy, DFIG, PI Controller, backstepping Controller, Active and reactive power control.

## I. INTRODUCTION

Non-renewable energies such as oil, nuclear power, natural gas, and coal have many drawbacks for mankind and the environment [1], and this has led researchers to find an alternative solution known as renewable energy [2]. Renewable energies are a natural alternative to conventional power generation. It is a clean, sustainable source of energy for power generation, and has received a great deal of attention in recent decades [3,4]. However, wind power is one of the most important sources of installed capacity worldwide [5,6]. Wind power is the most promising and the fastest-growing.

In the industrial market, the wind energy system based on the doubly-fed generator induction generator (DFIG) is the best-known and most usable system, thanks to several advantages [7]. One of its advantages is that the power transited by the two converters, on the rotor and grid sides, represents 30% of the total power supplied by the DFIG stator [6]. The DFIG's rotor winding is linked to the grid via a variable frequency converter, consisting of an

AC/DC converter situated on the rotor side (RS), a DC link capacitor, and a DC/AC converter situated on the grid side (GS). Direct grid connectivity exists between the DFIG's stator winding and grid [7]. The rotor speed can be adjusted in this setup to correspond with the wind speed [1-3].

With variable speeds, wind turbines can capture the maximum amount of power for each wind speed and run over a larger range of wind speeds. DFIG inverters are designed to only let through 25% of the rated power, in contrast to some synchronous machines that use their entire rated power to flow through the inverter [4].

Therefore, they are less cumbersome and more cost-effective [5,6]. It is difficult to extract the maximum power point for normal operation due to unstable environmental conditions and the non-linearity of the system caused by changes in wind speed [8]. To achieve this goal, maximum power point tracking and speed control techniques are used to increase the efficient use of wind turbines [9].

In the literature, there are different techniques for controlling energy systems, such as the

conventional controller and the advanced controller [5]. conventional controllers such as the proportional-integral (PI) are the most popular, but they have several drawbacks, because of their high damping, short response time, and lack of resilience against both internal and external disturbances, improved control techniques are becoming more and more important [10]. Intelligent control techniques including genetic algorithms, neural networks, and fuzzy logic are currently the focus of research, as well as non-linear control techniques like sliding mode and backstepping control, has led to some fascinating developments in the field of controlling renewable energy systems, particularly wind turbines and photovoltaic systems. The stability-based nonlinear control methods developed by Lyapunov, such as SMC and backstepping, continue to be a suitable middle ground that is reliable, simple to use, and provides high levels of satisfaction.

In this paper, two controllers have been presented to perfectly regulate the active power of the DFIG stator while also following variations in the maximum power extracted by the turbine through the regulation of the rotor-side converter. We juxtaposed and examined the two control approaches' responses to changes in the DFIG internal parameters to verify their ability to adapt. Below is the structure of this paper: Section 2 explains the DFIG-based wind-generating system. The DFIG is modeled using field-oriented control in Section 3. Section 4 covers the PI controller design and backstepping. Part 5 is dedicated to the presentation and discussion of the simulation results, with a summary of the study given in the last section.

## II. WIND ENERGY CONVERSION SYSTEM DESCRIPTION

A DFIG-based wind energy conversion system is shown in Figure 1. The wind energy system, which is transforms wind kinetic energy into mechanical energy and subsequently into electrical energy [11]. The mechanical part includes the turbine and gearbox, the electrical part consists of DFIG, and the control part uses two different types of controllers [12]. Two bidirectional AC-DC and DC-AC converters link the DFIG's rotor and stator to the grid, respectively, while two windings connect the stator directly to the grid. The main purpose of these converters is to change the frequency

between the grid and the generator rotor, enabling variable-speed operation of a wind turbine.

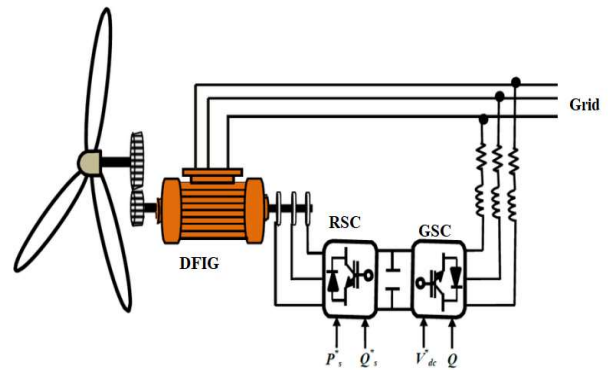


Fig.1. Wind energy conversion system based on DFIG.

## III. MODELING OF WIND ENERGY SYSTEM

Wind power is defined by Eq.1 [13]:

$$P_{aer} = \frac{1}{2} C_p(\lambda, \beta) \rho \pi R^2 V^3 \quad (1)$$

$$\lambda = \frac{\Omega_t R}{v} \quad (2)$$

The aerodynamic torque  $T_{aer}$  is given by Eq.3 [14,15]:

$$T_{aer} = \frac{P_{aer}}{\Omega_t} \quad (3)$$

The following two equations very simply model the multiplier:

$$T_g = \frac{1}{K} T_{aer} \quad (4)$$

$$\Omega_{mec} = K \Omega_t \quad (5)$$

The total inertia J is given by Eq.6:

$$J = J_g + J_t K^2 \quad (6)$$

The mechanical torque applied to the generator rotor is given by Eq.7:

$$T_{mec} = J \frac{d\Omega_{mec}}{dt} \quad (7)$$

The DFIG is modeled using the following assumptions: the air gap is constant, ferromagnetic losses are negligible, the influence of the skin effect and heating is not taken into account, and the notch effect is neglected [15,16]:

The rotor and stator voltage can be represented in the d-q rotating reference frame as shown in Eq.8:

$$\begin{cases} V_{ds} = 0 \\ V_{qs} = V_s = \omega_a \phi_{qs} \\ V_{dr} = R_r \cdot i_{dr} + \frac{d\phi_{rd}}{dt} - \omega_r \phi_{rq} \\ V_{qr} = R_r \cdot i_{qr} + \frac{d\phi_{rq}}{dt} + \omega_r \phi_{rd} \end{cases} \quad (8)$$

The stator current can be represented in the d-q rotating reference frame as shown in Eq.9:

$$\begin{cases} i_{sd} = \Phi_s/L_s + i_{dr} \cdot M/L_s \\ i_{sq} = -i_{qr} \cdot M/L_s \end{cases} \quad (9)$$

The stator flux can be represented in the d-q rotating reference frame as shown in Eq.10:

$$\begin{cases} \phi_{ds} = \varphi_s \\ \phi_{qs} = 0 \end{cases} \quad (10)$$

Stator reactive and active power can be represented as shown in Eq.11:

$$\begin{cases} P_s = -V_s \frac{M}{L_s} I_{qr} \\ Q_s = -V_s \frac{M}{L_s} I_{dr} + \frac{V_s^2}{L_s \omega_s} \end{cases} \quad (11)$$

#### IV. REACTIVE AND ACTIVE POWER CONTROL

In this study, the reactive and active power of the DFIG were regulated using two distinct regulators: proportional-integral controller (PI), and backstepping Controller (BAC).

##### A) Proportional integral Controller

PI corrector schematic diagram is shown in Figure 2. The transfer function of the conventional PI controller with the pole placement method is defined by Eq.12 :

$$T_F(p) = \frac{\frac{K_p}{P} \left( P + \frac{K_i}{K_p} \right)}{JP^2 + (F + K_p)P + K_i} \quad (12)$$

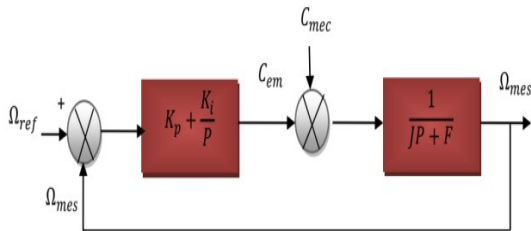


Fig. 2. PI corrector schematic diagram.

The gains of the correctors are presented in Eq.13:

$$\begin{cases} K_p = \frac{\sigma \cdot L_r L_s \cdot 2\omega_n \cdot \xi - R_r \cdot L_s}{M_{rs} \cdot V_s} \\ K_i = \frac{\sigma \cdot L_r L_s \cdot \omega_n^2}{M_{rs} \cdot V_s} \end{cases} \quad (13)$$

##### B) backstepping Controller

✓ *First Step: Control of Reactive and Active power*

The reactive and active power error and their derivation are defined by Eqs. (14) and (15):

$$\begin{cases} e_1 = P_{s-ref} - P_s \\ e_1 = P_{s-ref} - P_s \end{cases} \quad (14)$$

$$\begin{cases} e_3 = Q_{s-ref} - Q_s \\ e_3 = Q_{s-ref} - Q_s \end{cases} \quad (15)$$

The 1st Lyapunov candidate function is presented by Eq. (16):

$$\begin{cases} V_1 = \frac{1}{2} e_1^2 \\ V_3 = \frac{1}{2} e_3^2 \end{cases} \quad (16)$$

The derivative of the function (17) is given by Eq. (17):

$$\begin{cases} \dot{V}_1 = e_1 \dot{e}_1 = e_1 \left\{ P_{s-ref} - V_s \frac{M}{\alpha L_s} \left( V_{rq} + R_r I_{rq} + g\omega_s \left( L_r - \frac{M^2}{L_s} \right) I_{rd} - g \frac{MV}{L_s} \right) \right\} \\ \dot{V}_3 = e_3 \dot{e}_3 = e_3 \left\{ Q_{s-ref} - V_s \frac{M}{\alpha L_s} (V_{rd} + R_r I_{rd} - g\omega_s \alpha I_{rq}) \right\} \end{cases} \quad (17)$$

The derivative of the power errors becomes as shown in Eq. (18):

$$\begin{cases} \left\{ P_{s-ref} - V_s \frac{M}{\alpha L_s} (V_{rq} + R_r I_{rq} + g\omega_s (L_r - \frac{M^2}{L_s}) I_{rd} - g \frac{MV}{L_s}) \right\} = -K_1 e_1 \\ \left\{ Q_{s-ref} - V_s \frac{M}{\alpha L_s} (V_{rd} + R_r I_{rd} - g\omega_s \alpha I_{rq}) \right\} = -K_3 e_3 \end{cases} \quad (18)$$

The rotor currents references are expressed as shown in Eq. (19):

$$\begin{cases} I_{rq-ref} = \frac{\alpha L_s}{V_s M R_r} \left[ P_{ref} + k_1 e_1 \right] + \frac{1}{R_r} (V_{rq} - g\omega_s \alpha I_{rd} - g \frac{MV}{L_s}) \\ I_{rd-ref} = \frac{\alpha L_s}{V_s M R_r} \left[ Q_{s-ref} + k_3 e_3 \right] - \frac{1}{R_r} (V_{rd} - g\omega_s \alpha I_{rq}) \end{cases} \quad (19)$$

✓ *Second Step: Control of Rotor currents*

The rotor currents errors and their derivation are given by Eq. (20):

$$\begin{cases} e_2 = I_{rq-r} - I_{rq} \\ e_2 = I_{rq-r} - I_{rq} \end{cases} \quad (20)$$

$$\begin{cases} e_4 = I_{rd-r} - I_{rd} \\ e_4 = I_{rd-ref} - I_{rd} \end{cases} \quad (21)$$

The 2<sup>nd</sup> Lyapunov chosen function is defined by Eq. (22):

$$V_2 = \frac{1}{2}(e_1^2 - e_2^2), V_4 = \frac{1}{2}(e_3^2 - e_4^2) \quad (22)$$

The derivative of the function is given by Eq. (23):

$$\begin{cases} \dot{V}_2 = e_1 \left\{ P_{s-ref} - V_s \frac{M}{\alpha L_s} (V_{rq} + R_r(I_{rq-ref} - e_2) + g\omega_s \alpha I_{rd} - g \frac{MV}{L_s}) \right. \\ \quad \left. + e_2 \left\{ I_{rq-ref} - \frac{1}{\alpha} (V_{rq} + R_r(I_{rq-ref} - e_2) + g\omega_s \alpha I_{rd} - g \frac{MV}{L_s}) \right\} \right\} \\ \dot{V}_4 = e_3 \left\{ Q_{s-ref} - V_s \frac{M}{\alpha L_s} (V_{rd} + R_r(I_{rd-ref} - e_4) - g\omega_s \alpha I_{rq}) \right. \\ \quad \left. + e_4 \left\{ I_{rd-ref} - V_s \frac{M}{\alpha L_s} (V_{rd} + R_r(I_{rd-ref} - e_4) - g\omega_s \alpha I_{rq}) \right\} \right\} \end{cases} \quad (23)$$

with:

$$\alpha = L_r \delta = L_r \left( 1 - \frac{M^2}{L_s L_r} \right) \quad (24)$$

Then the reference rotor voltages are given by Eq. (25):

$$\begin{cases} V_{rq-c} = \left( -k_2 e_2 - I_{rq-ref} - \frac{V_s M R_r}{\alpha L_s} e_1 \right) \alpha - (R_r I_{rq} + g\omega_s \alpha I_{rd} + g \frac{MV}{L_s}) \\ V_{rd-c} = \left( -k_4 e_4 - I_{rd-ref} - \frac{V_s M R_r}{\alpha L_s} e_3 \right) \alpha - (R_r I_{rq} - g\omega_s \alpha I_{rd}) \end{cases} \quad (25)$$

## V. SIMULATION RESULTS

In this section, the comparison results between two regulators for active and reactive power control have been presented. We carried out a simulation using MATLAB/Simulink, to study the performance of the DFIG controlled by two controllers, the PI controller and Backstepping for power control. Figures 3 and 4 show the results of simulating wind energy conversion with power control by the conventional PI controller and by Backstepping mode as follows: (Fig. 3. a) torque, (Fig. 3. b) active power and its reference, (Fig. 3. c) reactive power and its reference, (Fig. 4.a) torque, (Fig. 4.b) active power and its reference, (Fig. 4. c) reactive power and its reference.

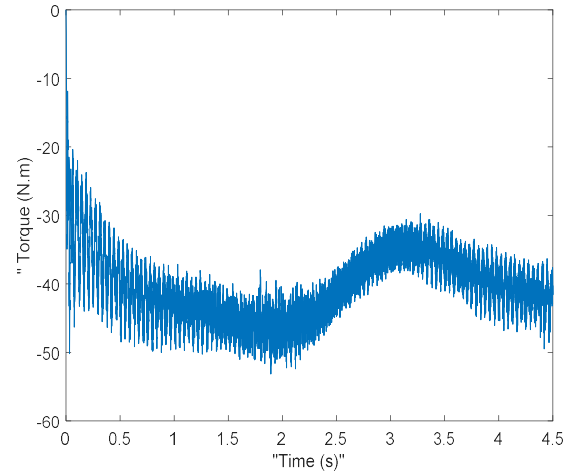
Figure 3. shows disturbances and fluctuations in the torque. According to Figure 3. b and Figure 3. c, active and reactive power follow their references perfectly, but the results contain the presence of abnormal fluctuations. So, we can see that the stator's active and reactive powers perfectly reach their reference profile, but with an accepted error, and that the electromagnetic torque profile follows its reference, but with a strong disturbance.

From Figure 4. a it is clear that torque takes the form of active power without disturbance.

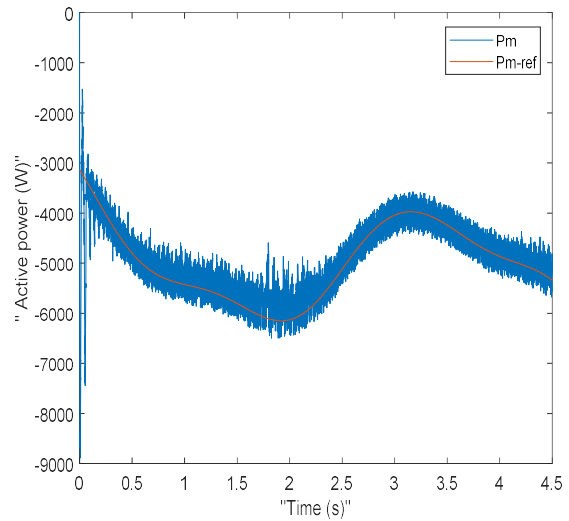
Figure 4.b and figure 4.c show that active and reactive power follow their references perfectly.

So we can say that the stator's active and reactive powers follow their reference profile perfectly when injected into the network and are completely decoupled and that the result of the electromagnetic torque about its reference is perfect and takes the same waveform as the active power with zero error.

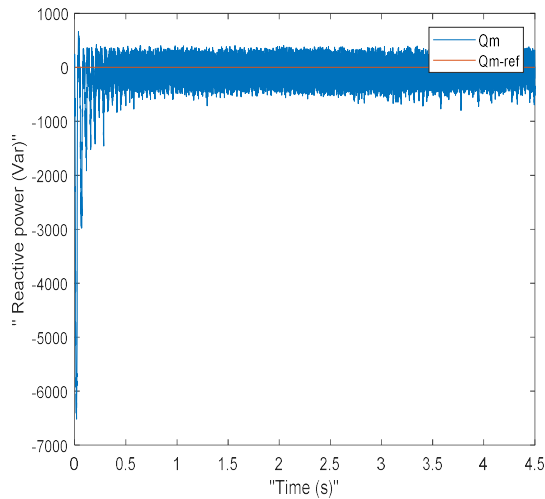
Thus, we can say that the simulation results confirm that MPPT control with mechanical speed control by the advanced controller is more efficient and robust than the conventional controller since the maximum power obtained by backstepping without exceeding the instruction is tracked identically in transient and steady-state conditions compared to the proportional-integral controller.



(a)

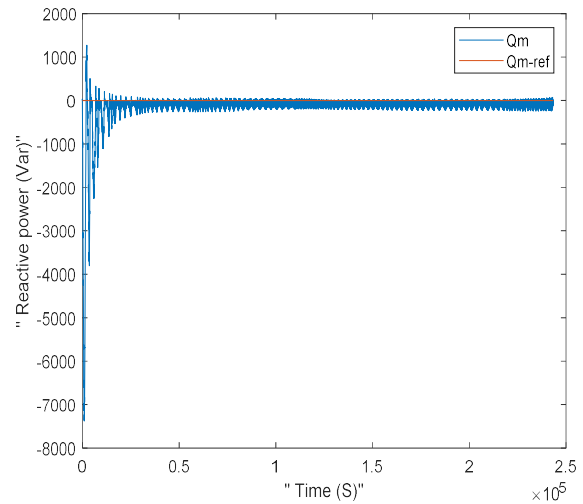


(b)



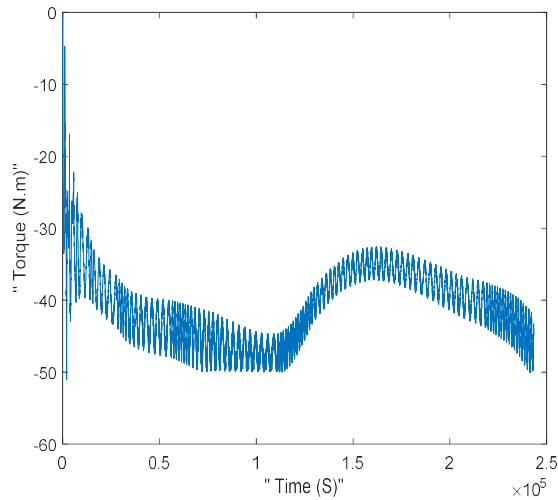
(c)

**Fig. 3.** MPPT command simulation with mechanical speed control using the PI controller.

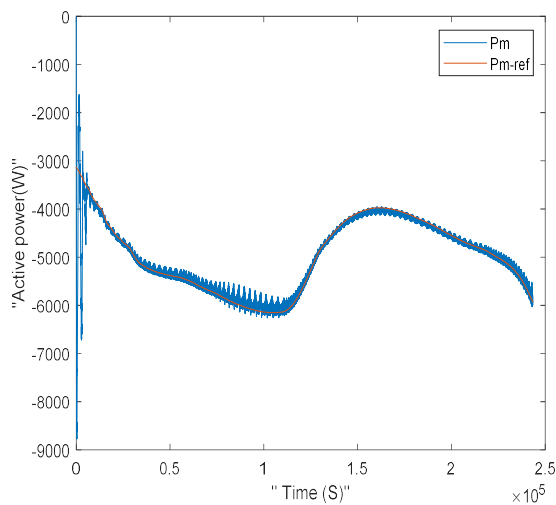


(c)

**Fig. 4.** MPPT command simulation with mechanical speed control using the BAC controller.



(a)



(b)

## VI. CONCLUSION

This work presents the modeling and control of a DFIG-based wind energy system using two different controllers under variable wind speed. Simulation results are synthesized and compared in the DFIG section, in terms of reference tracking and robustness, and have been presented in MATLAB/Simulink software. The results of the backstepping controller simulation showed high system stability and very fast response, with very low total harmonic distortion of the reactive and active power injected into the power grid.

The results show that the backstepping controller is more robust than the proportional-integral controller. Furthermore, the above results validate the efficacy of this non-linear backstepping control.

## VII. REFERENCES

- [1] M. A. Akbari, J. Aghaei, and M. Barani, "Convex probabilistic allocation of wind generation in smart distribution networks," *IET. Renew. Power. Gener.*, vol. 11(9), pp. 1211–8, 2017.
- [2] H. Afghoul, F. Krim, B. Babes, A. Beddar, and A. Kihal, "Design and real-time implementation of sliding mode supervised fractional controller for wind energy conversion system under sever working conditions," *Energy Convers. Manag.*, vol. 167, pp. 91–101, 2018.
- [3] A. Beddar, H. Bouzekri, B. Babes, and A. Afghoul, "Experimental enhancement of fuzzy fractional order PI + I controller of grid-connected variable speed wind energy conversion system," *Energy Convers. Manag.*, vol. 123, pp. 569–580, 2016.
- [4] N.T. Anh Tuyet, S.Y. Chou, "Maintenance strategy selection for improving cost-effectiveness of offshore

- wind systems,” *Energy Convers. Manag* 157, 86-95 (2018).
- [5] J.M. Adànez, B.M. Al-Hadithi, A. Jiménez, ”Wind turbine multivariable optimal control based on incremental state model,”*Asian J control* 20,1-13(2018).
- [6] V. Kumar, A. S. Pandey, S. K. Sinha, “Grid integration and power quality issues of wind and solar energy system,” a review. *In: International Conference on Emerging Trends in Electrical, Electronics and Sustainable Energy Systems (ICETEESSES-16), IEEE, vol. 11–12, March 2016.*
- [7] N Jargalsaikhan H Masrur A Iqbal S. Rangarajan S Byambaa T Senjyu, ” A control algorithm to increase the efficient operation of wind energy conversion systems under extreme wind conditions ” *J. Int. Energy Reports.* (8), 11429-11439 (2022).
- [8] S. Obukhov, A. Ibrahim, AA. Zaki Diab, AS. Al-Sumaiti, R. Aboelsaud, “(2020) Optimal performance of dynamic particle swarm optimization based maximum power trackers for stand-alone PV system under partial shading conditions”. *IEEE Access* 8:20770–20785.
- [9] D. Song, et al “Maximum power extraction for wind turbines through a novel yaw control solution using predicted wind directions”. *Energy Convers. Manag.* 157, 587–599 (2018).
- [10] Y. Dbaghi, S. Farhat, M. Mediouni, H. Essakhi, A. Elmoudden, “Indirect power control of DFIG based on wind turbine operating in MPPT using backstepping approach”, *International Journal of Electrical and Computer Engineering (IJECE) Vol. 11, No. 3, pp. 1951~1961,2021.*
- [11] M. Hoshyar, and M. Mola, “Full adaptive integral backstepping controller for an interior permanent magnet synchronous motor,” *Asian J. Control*, vol. 20, pp. 1–12, 2018.
- [12] S. Heier, *Grid integration of wind energy: onshore and offshore conversion systems: John Wiley & Sons, 2014.*
- [13] Y. Djeriri, H. Mesai Ahmed , M. Allam, « Commande par mode glissant de la GADA associée à un convertisseur à trois niveaux de tension à structure NPC et entraînée par une turbine éolienne », *First International Conference on Smart Grids, CIREI'2019 March 4-5, 2019 at ENP- Oran – Algeria.*
- [14] A. Boumassata D. Kerdoun O. Oualah,”Maximum Power Control of a Wind Generator With an Energy Storage System To Fix the Delivered Power”, *Electrical Engineering & Electromechanics*, (2), 41–46, 2022.
- [15] J. Salameh,” Active control approach for the optimization of wind turbine lifetime”, *D. thesis from the University of La Rochelle,2019.*
- [16] Y. Bekakra, D .Ben Attous, “ DFIG sliding mode control fed by back-to-back PWM converter with dc-link voltage control for variable speed wind turbine,” *Front. Energy*, vol. 8(3), pp. 345–354, 2014.